A COMPARISON OF POD AND TAIL MOUNTED RAMJETS

D.R.M. Arens[*] and H.V. Hattingh[**]
Propulsion Laboratory
University of Stellenbosch, Stellenbosch
7600 Republic of South Africa

Abstract

The practical feasibility of an annular, tail-mounted ramjet, which showed promise of being an effective propulsion concept for high speed remotely piloted vehicles, was investigated. The central tubular boundary layer duct did not present unsurmountable problems and a developed version of the engine was operated satisfactorily on a directly connected test bed installation, simulating supersonic operation at sea level.

Nomenclature

A   area
C   velocity
D   diameter
F   thrust
M   Mach number
$\dot{m}$ mass flow rate
p   pressure
T   temperature
ψ stability parameter

Subscripts:

b   boundary layer
e   engine
h   hydraulic
∞ free stream
1-7   engine sections as defined in figure 2

Introduction

In the development(1) of a computer program as a design tool for a hydrocarbon fuelled ramjet, permitting the selection of optimised parameters and the calculation of the performance of such engines, it was realised that the often very large engine in a long range application, resulted in an unwieldy flight vehicle. This is especially true with a single engine, as typified by a number of more or less successful designs over the years, from the V-1 of the 1940's to the North American Roadrunner of the 60's and more recent examples. When air release from an aircraft is considered, twin engines as in the Firebrand is possibly a better solution, allowing the missile or RPV to be carried close to the fuselage or wing of the carrier aircraft.

An interesting alternative is an integrated in-line tail mounted engine, as shown in figures 1 and 2. Such an installation has the advantage of lower drag, the base drag (wave drag, mostly) of the tail cone is obviated. It does, however, require the fuselage boundary layer to be internally ducted and virtually dictates a canard lay-out as shown in figure 1, which allows the fuel to be carried on or near the centre of gravity of the flight vehicle.
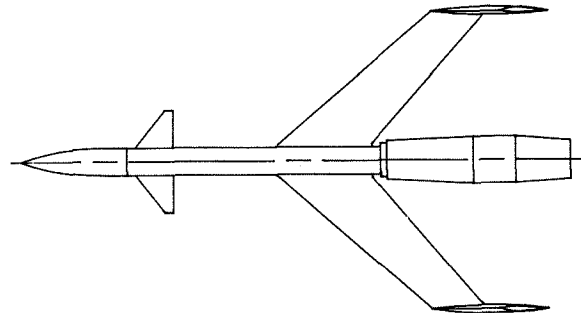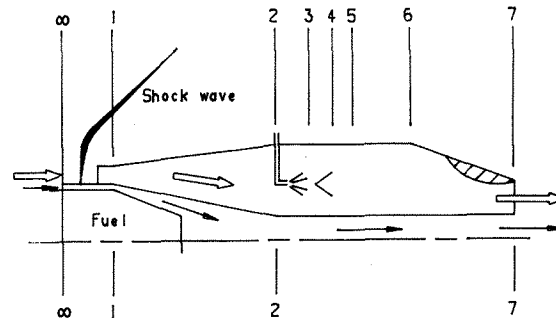
---

* Research Engineer
**Professor/Director

Figure 1. Integrated Tail Mounted Ramjet

∞ : Free stream
1 : Diffuser inlet
2 : Fuel injection
3 : End of mixing of air and fuel
4 : Flame stabiliser
5 : Beginning of combustion chamber
6 : Beginning of exhaust
7 : Exit

Figure 2. The Different Sections of the Engine

A multiple shock inlet of fixed geometry may be considered for such an engine, but variable geometry will be extremely difficult. To keep the investigation simple, the theory and computer programs(2) were developed to compare an integrated tail mounted engine with a pod mounted engine. Directly comparable results were obtained, figure 3, and justified a further investigation of the practical feasibility of the tail-mounted engine.

Figure 3. Computer Results

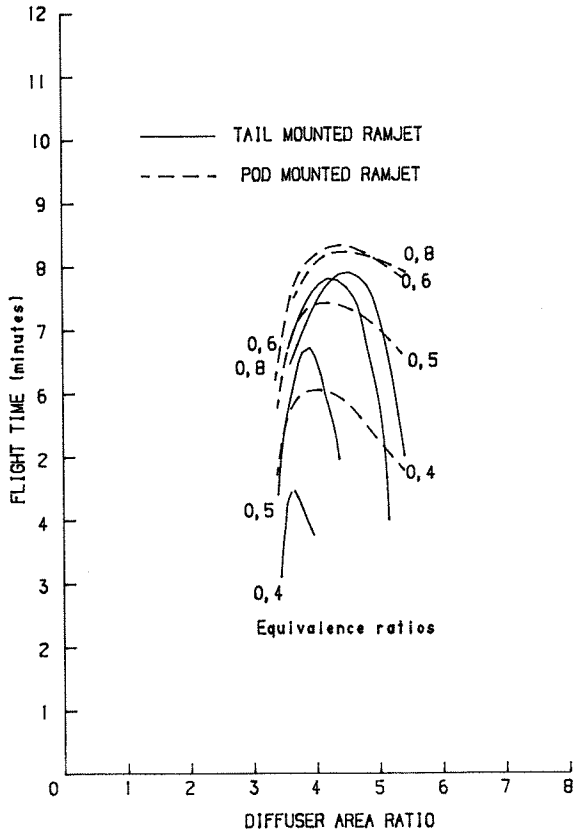of describing this, is to select the Mach number at the outer edge of the bleed. The flow in the real engine may then be modelled as shown in figure 4. In the directly connected engine the flow after the terminal shock (of variable strength) and mixing of the flow to yield average conditions, is modelled, figure 5.
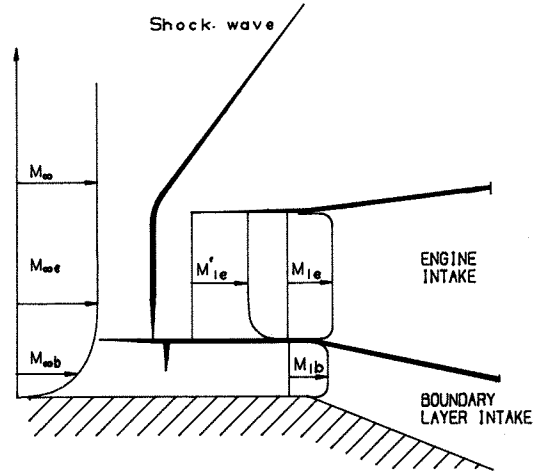

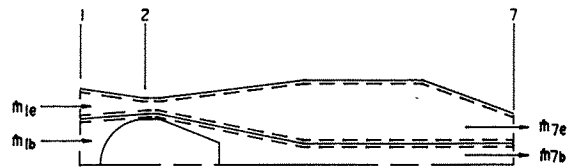Figure 4. Boundary Layer Intake Model

Figure 5. Model for Thrust Calculation of Test Ramjet

For the design of the test engine a Mach number of 1,2 was selected at the outer edge of the boundary layer bleed, with M_∞ = 1,4, resulting in 30% bleed flow.

Experimental Engine

The same design data was used for the design of the flameholders and combustion chambers of both engines, pod and tail mounted.

The presence of the centrally situated boundary layer duct is, however, a disturbance.

It changes a cylindrical combustion chamber into an annular chamber with two walls on which fuel may be deposited with, possibly, resultant incomplete combustion. Combustion stability may also be affected.

A typical design was chosen to be tested on a test-bed in direct connect mode. Limitations on the air mass flow available to the particular test-bed necessitated the use of a smaller than typical test engine. The following, refer also to figure 2, applied:

Design flight Mach number: 1,4
Design flight altitude : Sea level
Stabiliser blockage : 70%

One of the variables in the optimisation is the amount of boundary layer bled off. Another way

Test Bench

The air is supplied to the test engine via a vitiated air preheater, figures 6 and 7.

A combustion chamber from a JT-8 engine is used, mounted in a bulkhead and surrounded by bypass valves. Dividing the flow permits the combustion chamber to be operated at optimal conditions. The heated and cold air streams are mixed before flowing into the settling chamber.
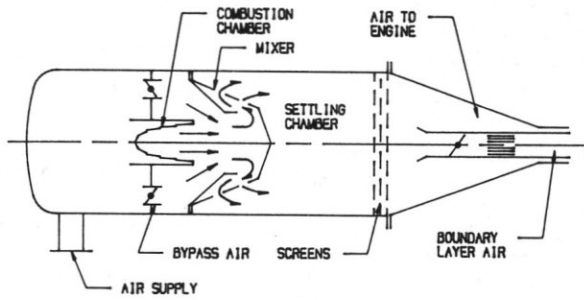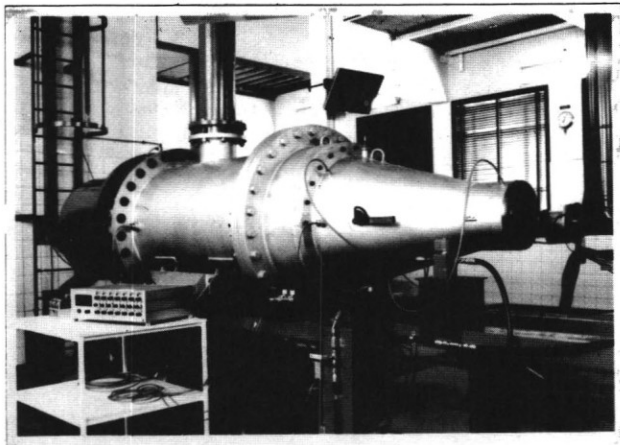
Figure 6. Internal Flow of Preheater

Figure /. Preheater

The air, now at the .desired $T_{o\infty}$ as measured in the settling chamber by four thermocouples, flows through screens in the settling chamber into a contraction, figure 6, at the outlet of which a sliding seal joint is provided with the test engine. The main or engine air flow in the outer annulus visible in figure 7 will be at the stagnation pressure measured in the settling chamber, which is controlled at the required value corresponding to the flow conditions shown in figure 4. The boundary layer flow will be at a lower stagnation pressure, which is obtained by throttling the air supply to the central circular outlet by means of a perforated butterfly valve. The flow profile downstream of the valve is smoothed by a further set of three screens, figure 6.

For practical reasons, easing the installation of the seals, the test engine has a larger inlet diameter than the real engine. This construction causes a difference in thrust between the real engine and the experimental engine; the control volume over which the difference of entry and exit momentum is computed, differs from the control volume in the optimisation program(2).

This difference is taken into account by measuring the static pressure at the intake of the engine, both in the main air flow and the boundary layer flow. The static pressure at the connection between the engine and the preheater is also measured.

The total mass flow is determined with an orifice in the air supply line to the preheater. Knowing the main air flow, the boundary layer mass flow is calculated and with the appropriate measured pressures and stagnation temperature, the respective velocities at sections 1 and 2, see figure 5, are determined. With these values the momentum change due to the connection section can be calculated and brought into account for the thrust calculation of the real engine.

Measured thrust:

$$F_m = \dot{m}_{7e} \cdot C_{7e} + \dot{m}_{7b} \cdot C_{7b} - \dot{m}_{1e} \cdot C_{1e} -$$
$$\dot{m}_{1b} \cdot C_{1b} - (p_1 - p_\infty) \cdot (A_{1e} + A_{1b}) \quad (1)$$

Calculated thrust for the real engine:

$$F_c = \dot{m}_{7e} \cdot C_{7e} + \dot{m}_{7b} \cdot C_{7b} - \dot{m}_{1e} \cdot C_{2e} -$$
$$\dot{m}_{1b} \cdot C_{2b} - (p_{2e} - p_\infty) \cdot A_{2e} - (p_2 - p_\infty) A_{2b} \quad (2)$$

Change of momentum for connection section:

$$\Delta F_c = (p_{2e} - p_\infty) \cdot A_{2e} + (p_{2b} - p_\infty) \cdot A_{2b} +$$
$$\dot{m}_{2e} \cdot C_{2e} + \dot{m}_{1b} \cdot C_{2b} - (p_{1e} - p_\infty) \cdot A_{1e} -$$
$$(p_{1b} - p_\infty) \cdot A_{1b} - \dot{m}_{1e} \cdot C_{1e} - \dot{m}_{1b} \cdot C_{1b} \quad (3)$$

It is obvious that by subtracting equation (3) from equation (1), the measured thrust of the real engine is obtained, and can now be compared with the theoretical thrust.

Experimental Results

The experimental engine, figure 8, was constructed in such a way that modifications could be introduced with relative ease. The fuel supply manifold feeding three supply spokes to the fuel spray bar illustrates this approach.
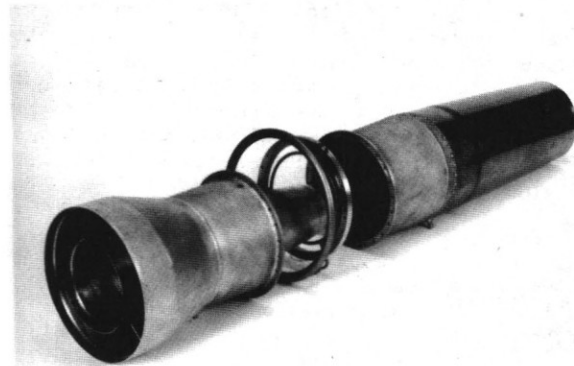

Figure 8. Different Modules of Engine

Ignition

The engine was ignited by means of a torch igniter, which simulated a pyrotechnic device. Four different locations were experimented with:

1. *Immediately Downstream of the Flame Holder:*
    The air-fuel mixture ignited, but the flame did not attach to the flame holder. As soon as the ignitor was switched off, combustion ceased.

2. *Upstream of the Flame Holder, Immediately Downstream of the Fuel Injection Ring:*
    The results were better, the flame attaching to the flame holder. But there was also a flame behind the torch ignitor (it was acting as a flame holder), partially immersing the true flame holder in combustion products.

3. *Immediately Upstream of the Flame Holder:*
    A further improvement, flame now correctly anchored.

4. *Inside One of the Radial Stabiliser Struts:*
    The torch igniter was mounted inside one of the radial struts of the flame stabiliser, so as to integrate the igniter with the flame stabiliser.

This configuration proved to be satisfactory.

Scale Effect

During the first tests a combustion instability was noticed at quite low air flow rates, already. It was realised that the engine had been designed for a larger mass flow rate and thrust, and was then directly scaled down to suit the lower available mass flow. In the process the double rings of concentric V-gutter flame stabilisers were made too small, limiting the range of stable combustion.

The two rings of small gutters were replaced by one ring of greater width, but same total projected area. This immediately yielded improved stability.

Fuel Injection

A further increase in air mass flow towards the design point resulted in renewed instability. The simple multiple hole (of 0,5 mm diameter) fuel injector ring was considered the likely culprit. Variations of this injector configuration were experimented with, varying the direction of injection from downstream, to radial or combined downstream and radial and upstream only. The latter produced the worst results, causing fuel to form a film on the walls. Even at high, near design point, air mass flow rate and with combustion the film of fuel on the outer wall was clearly visible as it left the nozzle as a mist of fuel surrounding the exhaust flame.

Eight, and later ten, simplex type swirler *fuel injectors, mounted on the fuel ring and* facing downstream, yielded the best stability results. This configuration was adopted for the further tests of this engine, but is should be noted that it is believed that the *small size* of the engine was the root cause of the unsatisfactory atomisation achieved; a larger engine would also have a larger diffuser in which the fuel would more readily atomise and mix with the air.

Liners

One of the main causes of the combustion instability was the unlined walls of the combustion chamber and exhaust with the associated films of fuel on these walls, which did not take part in the combustion. This was proved by testing with different engine geometries.

The first step was to look at the combustion process without the outer combustion chamber wall and exhaust nozzle, retaining the full length of the central boundary layer duct, but with the design air mass flow. This yielded stable combustion, and proved that the *high velocity* at the flame holder was not the cause of the instability, but that interaction with the wall was the problem. The next step was to connect a cylindrical exhaust without liner, which resulted once more in instability. To prevent this, a liner was installed, consisting of a non-perforated section from the fuel injection ring to the flame stabilisers, and then a perforated section (17,5% of total area) to the end of the exhaust nozzle, leaving a gap between the liner and the engine wall, so that air could flow between the wall and the liner. The non-perforated section of the liner prevented the formation of a fuel film on the engine wall, figure 9.
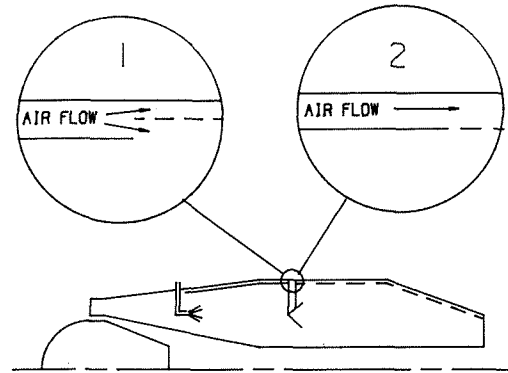

Figure 9. Different Connections for Liner

Two types of connection between the non-performated section and the perforated section of the liner were used. The first connection was an open type of connection, see figure 9, case 1. The fuel which formed a film on the wall of the non-perforated section was blown away at the connection. This was done by air that flowed out of the gap between the liner and engine wall, back into the main air flow.

The solution improved the range of stability substantially.

The inner wall, the boundary layer duct, is difficult to treat in such a way, but did not seem to *have a serious effect, possibly* because of its smaller area.

Three localised combustion zones formed between the outer wall and the liner, behind the three V-shaped struts carrying the flame stabiliser. This was obviated by streamlining the struts between the outer wall and the liner.

Stability Curves

With combustion stability over as wide a range of operating conditions as possible being of prime importance, the test results during this development phase were plotted as values of the combustion parameter at which stable combustion was maintained against fuel air ratio.

The combustion parameter is defined as

$$\psi = C_2/(T_2^{1,5} \cdot P_2^{0,95} \cdot D_h^{0,85}) \qquad (4)$$

The results for the original engine design, with the outer combustion chamber casing removed, is shown in figure 10. A limited range of stable operation was achieved, unexpectedly on the lean side of the "standard curve" based on tests with a homogeneous mixture of gas and air and a round disc flame stabiliser.
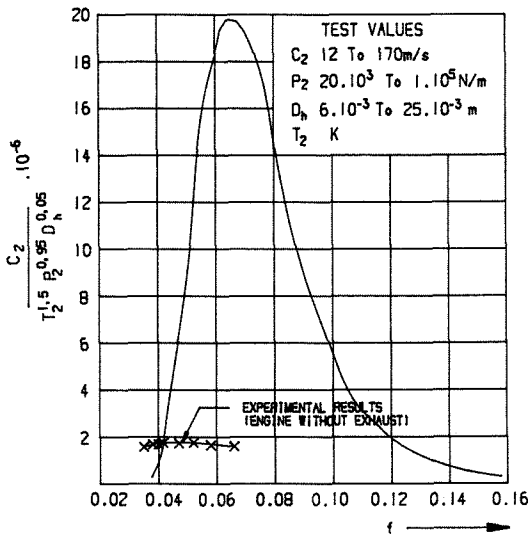

Figure 10. Experimental Results

The revised engine with the modifications described above yielded the much wider operating range shown in figure 11. The combustion parameter changes very little as the engine "accelerates" on the test bed, because of the gasdynamic relationship between pressure and velocity, which tends to cancel the effect of changes in these parameters on the stability parameter.
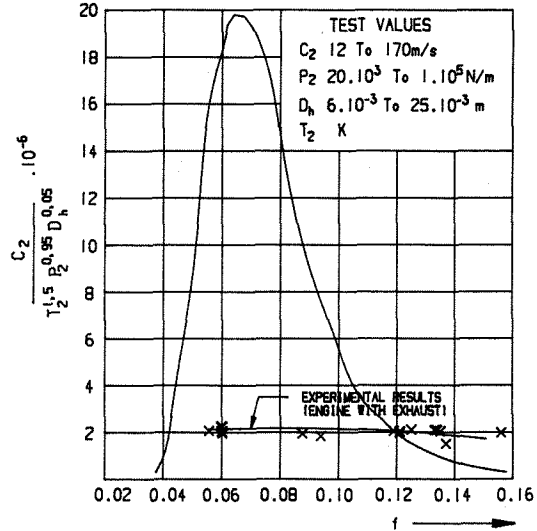

Figure 11. Experimental Results

Conclusions

The tail-mounted annular ramjet was shown to operate satisfactorily and further tests to measure its performance and to correlate these results with the theoretical predictions will now be undertaken.

To obtain meaningful results the exhaust temperatures must be measured, as well as the simpler measurements of thrust, pressures, inlet temperature and air and fuel mass flows. Thermocouples may only be used for measurement of the exhaust temperature when very low values of equivalence ratio are used.

For this work and to satisfy similar requirements in other programs in the Propulsion Laboratory, an optical temperature measurement system has been acquired.

References

1. Hattingh H.V., "Cruise Flight Duration of a Low Mach Number Ramjet", AIAA 79-7040 R, Journal of Aircraft, June 1981, p. 425.

2. Hattingh H.V., Arens D.R.M. and van Wyk J.S., "Cruise Flight of a Tail Mounted Ramjet", 6th ISABE, Paris, June 1983.